AIAA JOURNAL
Vol. 30, No. 2, February 1992

Control of Jet Structure by Crown-Shaped Nozzles

Ellen K. Longmire,* John K. Eaton,† and Christopher J. Elkins‡
Stanford University, Stanford, California 94305

Flow visualization and hot-wire anemometry were used to examine the effects of indeterminate-origin nozzles on flow in the near field of an otherwise axisymmetric air jet. The jet Reynolds number based on nozzle exit diameter was 19,000. Flow structure was investigated under both unforced and forced conditions where the forcing frequency corresponded to a Strouhal number based on diameter of 0.51. Time-averaged views of the unforced flow showed significant deviations of the jet from axisymmetry. Phase-averaged slices of forced flow strobed with a copper vapor laser revealed strong variations in entrainment along different azimuthal planes. Also, the phase-averaged visualizations showed repeatable coherent longitudinal vortex structures attached to the larger-scale vortex rings normally observed in round jets. When tooth length and number on the nozzle attachments were varied, the stability and propagation patterns of these longitudinal structures could be altered.

Nomenclature

D = jet exit diameter
E_{uu} = power spectral density function for axial velocity fluctuations
f = forcing frequency
Re_D = Reynolds number, UD/ν
r = radial coordinate
St_D = Strouhal number, fD/U
U = mean nozzle exit velocity
U_x = mean axial velocity
u'_x = rms axial velocity
x = axial coordinate
β = azimuthal angle
δ_ω = shear-layer vorticity thickness
ν = kinematic viscosity

Introduction

THE importance of vortex ring structures in the near field of round jets has been well documented. Attempts to control jet development have focused on perturbing the vortex rings by either active or passive means. This paper describes the near-field development of jets emerging from round nozzles with "indeterminate origins." The nozzles, illustrated in Fig. 1, have the shape of a crown with either 2, 4, or 8 peaks. The purpose of the crown-shaped nozzle is to introduce three dimensionality into the vortex rings at their origin thereby modifying the near field of the jet.

A number of experimenters have attempted to passively control jet structure by altering jet nozzle outlet geometries to induce three dimensionality. Ho and Gutmark[1] studied an elliptic jet with a 2:1 aspect ratio. The elliptic vortices that formed in the jet became distorted azimuthally due to self-induction causing greatly increased entrainment near the minor axis plane. The total entrainment in the near field was several times higher than that in a round jet. Schadow, et al.[2] examined the structure in a triangular jet. They found that coherent large-scale structures formed only along the triangle's sides. Near the vertices, however, small-scale eddies were dominant. Small-scale mixing was enhanced in these regions. Bradbury and Khadem[3] inserted small rectangular tabs into a round nozzle exit partially blocking the oncoming flow. The tabs caused decreased mean axial velocities and increased axial turbulence intensities along the jet centerline as well as strong deviations from axisymmetry in the mean axial velocity contours.

The term "indeterminate origin" was first used by Kibens and Wlezien[4] and Wlezien and Kibens[5] to describe nozzles in which the cross section was round, but the axial position of the nozzle exit varied around the circumference. In these two studies, inclined and stepped nozzle attachments were examined in forced and unforced flow. All of the nozzles caused distinct deviations from axisymmetry in the mean velocity contours, with forcing enhancing the deviations. In general, jet spreading increased in the azimuthal plane of symmetry of the nozzles and decreased perpendicular to the plane of symmetry. In nozzles with small angles of inclination, vortex rings tended to align with the nozzle exit, but in nozzles with greater angles of inclination, the rings aligned perpendicular to the jet axis. Krishnappa and Csanady[6] also studied indeterminate origin nozzles where triangular tabs (termed "vortex generators") were affixed to a round nozzle exit. Only the jet far field was examined. The vortex generators were found to reduce overall noise intensity without creating any variations in the directional distribution of the intensity.

The objectives of the present study were to examine both the mean flow development and the structural features of the jet emerging from the crown-shaped nozzles. The nozzles were expected to produce vortex rings with several kinks around the circumference. The questions to be answered then were how strong would these kinks be, and how would they affect jet mixing and growth?

Facility

Flow experiments were conducted in the facility depicted in Fig. 2. Air from a compressor was fed into a 5.08-cm (2 in.) diam plenum through opposing jet outlets. The flow passed vertically downward through a perforated plate before being accelerated through a 6.45:1 area ratio axisymmetric contraction with an exit diameter of 2 cm. Any of a set of five crown-shaped nozzles or an axisymmetric reference nozzle (see Fig. 1) could be appended to the contraction exit. The nozzles are labeled 2PL, 2PM, 2PS, 4P, 8P, and REF in subsequent figures and descriptions. All nozzles, which were machined from

Received Nov. 28, 1990; presented as Paper 91-0316 at the AIAA 29th Aerospace Sciences Meeting, Reno, NV, Jan. 7–10, 1991; revision received April 18, 1991; accepted for publication April 18, 1991.

*Research Assistant, Department of Mechanical Engineering; currently Assistant Professor, Department of Aerospace Engineering and Mechanics, University of Minnesota, Minneapolis, MN. Member AIAA.

†Associate Professor, Department of Mechanical Engineering, Member AIAA.

‡Research Assistant, Department of Mechanical Engineering. Student Member AIAA.

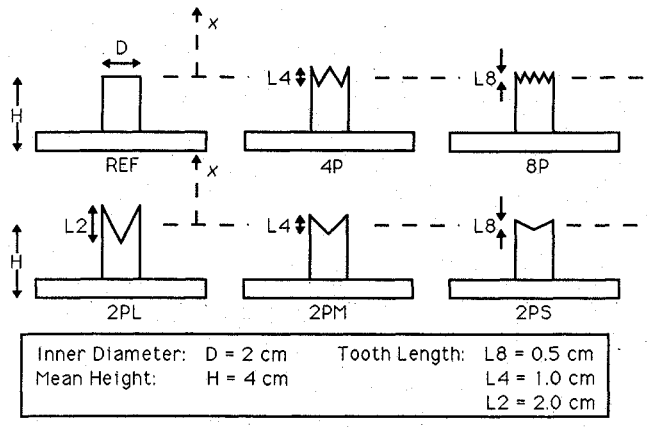

Fig. 1 Crown-shaped nozzle attachments.

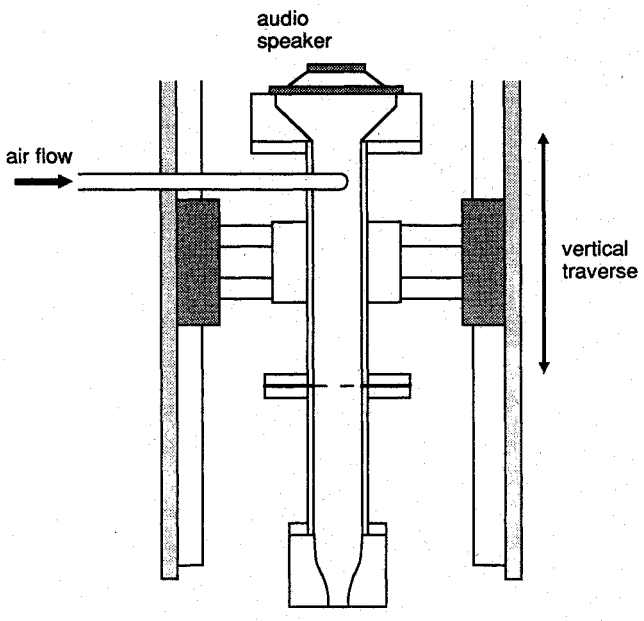

Fig. 2 Jet facility.

$^3/_4$ in. PVC pipe, had wall thicknesses of 1 mm on the downstream ends and inner diameters of 2 cm to match the contraction outlet. On the crown-shaped nozzles, the downstream edges were machined so that the local nozzle height varied directly with azimuthal angle. Thus, if the nozzle were "unwrapped," the downstream edges would appear as zigzagged line segments. Air flowing from the reference nozzle was found to have a top-hat-shaped velocity profile with a shear-layer vorticity thickness measured at $x/D = 0.05$ of 0.6 mm. Velocity fluctuation intensities at the jet exit centerline were approximately 10% of the mean.

An ordinary audio speaker located on top of the plenum could be used to force the flow strongly at specific frequencies to organize vortex ring structures rolling up in the shear layer downstream of the nozzle exit. An IBM XT computer containing a Data Translation 2801 data acquisition and control board generated the desired forcing waveforms that were low-pass filtered and fed through an amplifier before reaching the speaker. This system produced centerline velocity fluctuation intensities at the nozzle exit of 11% and 2% for forcing frequencies of 364 Hz ($St_D = 0.51$) and 556 Hz ($St_D = 0.78$), respectively. The forcing amplitudes were chosen as large enough to cause the roll up of vortex ring structures at the forcing frequency in the REF nozzle. Spectra of the axial velocity fluctuations taken at this location were completely dominated by a sharp peak at the forcing frequency. The most unstable frequency was estimated as 1700 Hz by using the shear-layer thickness at the nozzle exit. Any influence from this frequency was overwhelmed by the response from the forcing frequency. A more complete description of the experimental facility can be found in Longmire and Eaton.[7]

Diagnostics

Diagnostics employed for the flow studies were hot-wire anemometry and flow visualization. Axial flow velocities were measured with a single-wire TSI 1210 hot-wire probe on a 30.5 cm support (TSI 1150-12) connected to a TSI 1050 constant-temperature anemometer. The probe and support formed an angle of 45 deg with the jet axis, with the probe pointing toward the nozzle exit. Mean and fluctuating velocity values were determined from sets of 4000 samples taken at 400 Hz. Individual power spectral density functions were computed from 52 sets of 1024 samples taken at 5000 Hz. Since it is well-known that measurements made with a single hot wire in the jet shear layer contain significant biasing errors (see Tutu and Chevray[8]), the results reported here are used only for purposes of comparison.

A pulsed 10-W copper vapor laser was used for the flow-visualization studies. The beam was formed into either a vertical or a horizontal sheet to examine thin slices of the flow. Glycerine smoke was fed into the flow upstream of the jet plenum so that all flow issuing from the jet was seeded. The laser pulsing was controlled by the computer and coupled with the jet speaker forcing to create a strobing effect or a single phase-locked pulse. Strobed and instantaneous flow were captured on both videotape and 35-mm film. These techniques are described further in Longmire and Eaton.[7]

Results

Unforced Flow

Profiles and spectra were taken in different azimuthal planes for three crown-shaped nozzles as well as the round reference nozzle at $x/D = 1$, 2, 3, and 4. The axial coordinate x originates at the downstream edge of the REF nozzle or halfway between the peaks and troughs for the crown-shaped nozzles. The azimuthal angle β is defined such that $\beta = 0$ deg is always aligned with a nozzle peak. Jet Reynolds number based on a mean nozzle exit velocity of 14.4 m/s was 19,000.

Three velocity profiles were measured at each axial position for the 2PL, 2PM, and 4P nozzles. The azimuthal planes studied were the peak-to-peak (P) plane, the trough-to-trough (T) plane, and the plane midway between the previous two (I). Normalized profiles of mean and fluctuating velocity for the 2PL and REF nozzles are presented in Figs. 3 and 4. At $x/D = 1$, the mean and fluctuating profiles in the T plane are clearly further developed than the I or P profiles. This behavior is consistent with the idea that, at this axial position, the shear layer has developed over a distance of $1.5D$ in the T plane, which is three times greater than the $0.5D$ development distance in the P plane. The REF profiles differ significantly from the I profiles, however. Note that beyond r/D of 0.45, the intermediate plane mean velocity exceeds the reference mean by as much as 20% of the centerline velocity. Also, the maximum value of the fluctuating velocity in the I plane is 18% lower than that for the REF nozzle. Looking further downstream, we see that the mean profiles for the four cases lie closer together. The fluctuating profiles in the intermediate plane, however, continue to peak at lower values than the profiles in the P, T, or REF planes. Velocity profiles of flow from the 2PM and 4P nozzles show similar trends as those above.

The shear-layer vorticity thickness δ_ω was computed for each of the profiles displayed in Fig. 3, where δ_ω represents the local jet centerline velocity U_{cl} divided by the maximum slope dU/dr. The maximum slope was found by fitting lines to sets of four adjacent points within each profile. Figure 5 shows the resulting trends. A comparison of the data in the P and T planes shows that, in the P plane, δ_ω starts off smaller but grows at a faster rate until at $x/D = 3$ it overtakes the corresponding

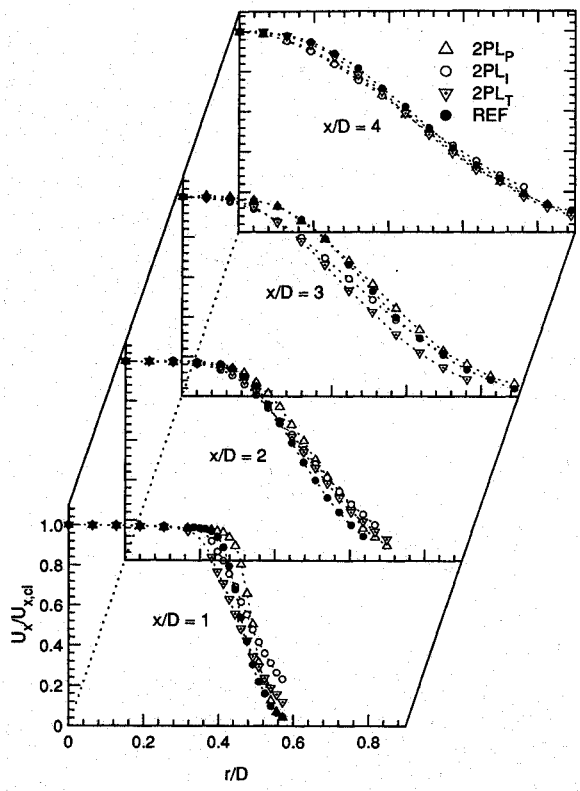

Fig. 3 Mean axial velocity profiles for 2PL and REF nozzles (x/D = 1–4).

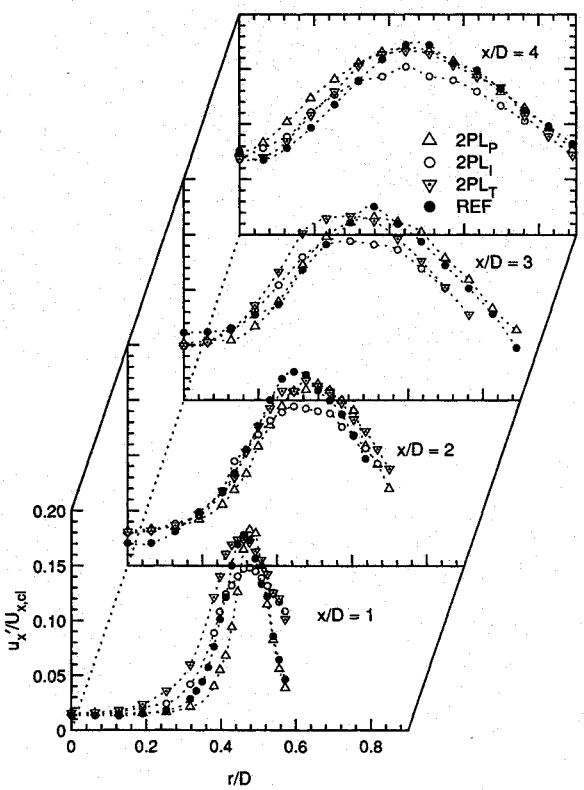

Fig. 4 Rms axial velocity profiles for 2PL and REF nozzles (x/D = 1–4).

value in the T plane. This trend matches that seen by Wlezien and Kibens[5] who determined shear-layer momentum thicknesses for flow from an inclined nozzle. The value of δ_ω in the I plane is generally larger than that seen in either the P or T planes. This result is opposite to that seen by Wlezien and

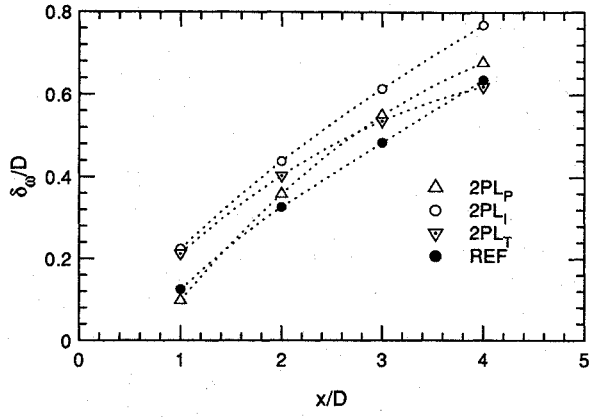

Fig. 5 Shear-layer vorticity thickness for 2PL and REF nozzles (x/D = 1–4).

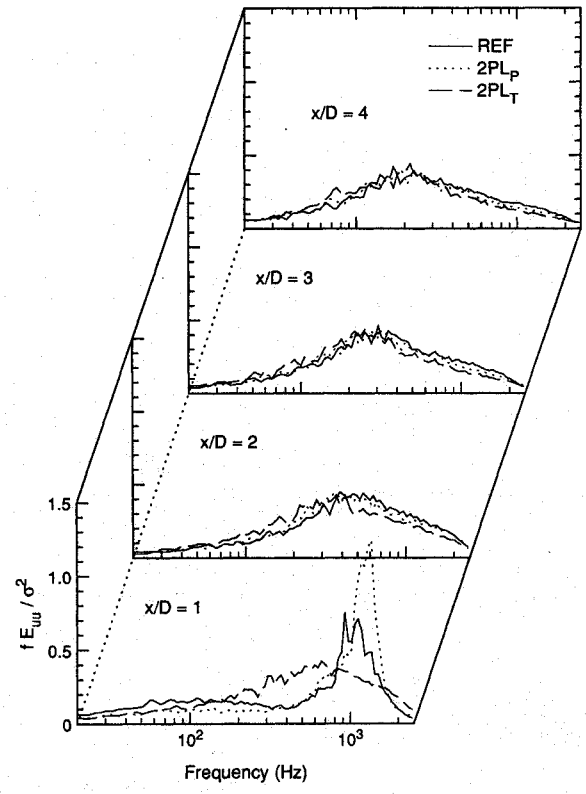

Fig. 6 Normalized power spectra for 2PL and REF nozzles (x/D = 1–4, r/D = 0.44).

Kibens in the inclined nozzle where the I plane yielded the smallest shear-layer thickness. It should also be noted that over the range plotted, the shear-layer thickness for the REF nozzle is smaller than that in any of the three azimuthal planes measured for the 2PL nozzle. The above results indicate that the crown-shaped nozzles cause significant deviations from the REF case, but give little idea of the mechanisms for the deviations.

Normalized power spectra of the axial velocity fluctuations were computed for the P and T planes of the 2PL, 2PM, and 4P nozzles as well as for the REF nozzle at x/D = 1–4. In all cases, the hot wire was positioned at r/D = 0.44, a location near the center of the shear-layer region. Spectra for the 2PL and REF nozzles are plotted in Fig. 6. At x/D = 1, the normalized plot of E_{uu} for the REF nozzle shows a distinct peak centered at 1100 Hz. The corresponding plot for the P plane in the 2PL case has a more distinct peak at 1300 Hz. In the T plane, however, the energy content is distributed over a wide range of frequencies with a weak peak at 680 Hz. Thus, the flow appears more developed in the T plane of the 2PL

case than in the corresponding P plane or the REF case. The same trend occurs for the 2PM and 4P nozzles at $x/D = 1$.

Beyond $x/D = 1$, the frequency content appears very similar for the different cases shown (as well as for the 2PM and 4P cases studied). At each axial position ($x/D = 2$, 3, and 4), all spectra are broadband and lie almost on top of each other. Since the spectra of the axial flow velocity do not vary azimuthally, it appears that by $x/D = 2$, the dominant axial structures in the flow span the nozzle circumference.

Time-averaged smoke visualizations of axial slices of flow from the 2PL, 2PM, 4P, and REF nozzles are depicted in Fig. 7. For each photograph, the laser was pulsed at 1920 Hz for a period of 1/30 s. An interesting characteristic of these photographs is that in the peak planes the nozzle exit fluid does not begin to spread for a distance of $0.6D$ downstream of the nozzle tips. The interface between the smoke-marked and outer fluid is sharp, implying that no intermittent fluctuations or structures occur over this distance. At $x/D = 0.6$ then, the jet suddenly spreads sharply in each case. If we define a spreading angle as the angle between the edge of the smoke-marked fluid and the jet axis, the spreading angles at $x/D = 0.6$ for the 2PL, 2PM, and 4P nozzles measure 18.5, 17, and 16 deg, respectively. The fluid from the REF nozzle spreads at about 0 deg until $x/D = 0.7$ when the angle increases to 15.5 deg. The spreading of the jet in the T planes near the nozzle exits appears different from that in the P planes. In the 2PL and 2PM cases, fluid exiting the troughs first spreads at about 2 deg for a distance of $0.7D$. Next the spreading angle increases to 10 deg. The spreading angle at this point for the 4P nozzle is 9 deg. Over the first $0.7D$ in the T planes, the interface between smoke-marked and outer fluid is not as sharp as in the P planes indicating the presence of intermittency. This difference and the difference in measured spreading angle between the P and T planes indicate that the shapes or sizes of structures rolling up in the jet near field vary azimuthally.

To examine the instantaneous structures in the unforced jet, axial slices of flow were also exposed to single laser pulses (30 ns). Examples of these photographs are shown in Figs. 8 and 9 for the 2PL and 8P nozzles. Each photograph shows evidence of vortical structures. Note the more coherent structures in the two photos of the 8P nozzle when compared with those seen in the 2PL nozzle. In the 8P case, distinct vortex cores, which have rolled up in the shear layer, are present. Evidence of coherent structures exists out to $x/D = 3.9$ in both the P and T planes. In the 2PL case, however, no distinct vortex cores are present beyond $x/D = 1$ in the T plane or $x/D = 2$ in the P plane. Note that in the 8P case, the small structures rolling up near the nozzle exit are of the same length scale as the tooth length, but in the 2PL case, the tooth length is approximately three times the original vortex length scale. It is unclear whether these original structures ever form coherent rings. Differences in jet structure due to azimuthal orientation are also unclear since each photograph represents only one instant in time.

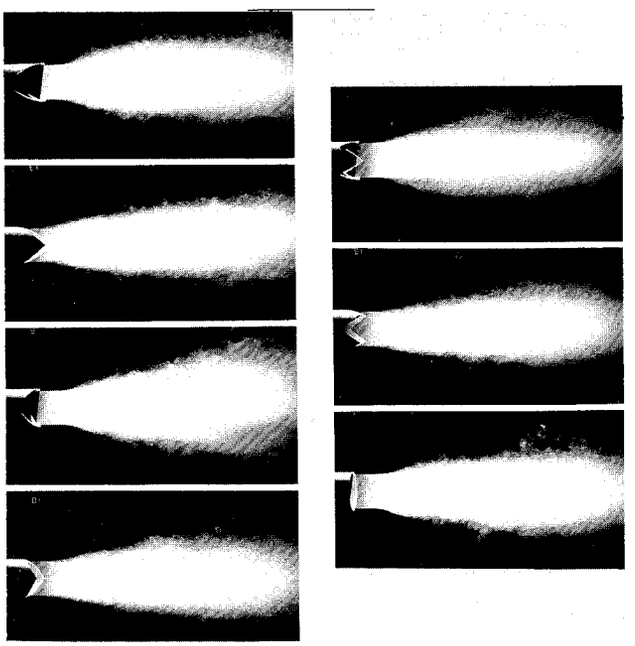

Fig. 7 Time-averaged smoke visualization of 2PL, 2PM, 4P, and REF nozzles (unforced, axial cuts).

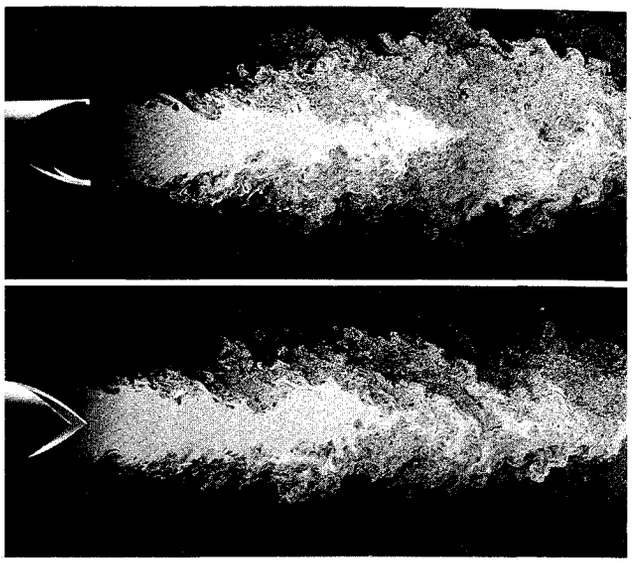

Fig. 8 Instantaneous smoke visualization (2PL nozzle, unforced).

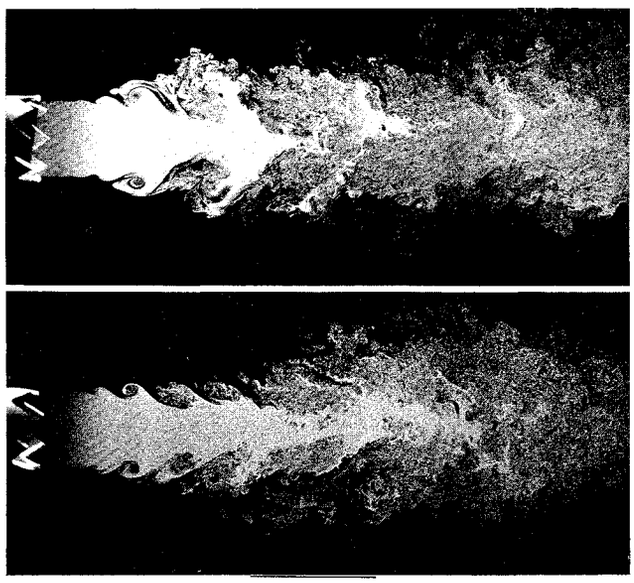

Fig. 9 Instantaneous smoke visualization (8P nozzle, unforced).

Forced Flow

The flow structure could be studied more systematically by forcing the jet and looking at phase-averaged results. A baseline forcing frequency of 364 Hz, which corresponds to a Strouhal number based on mean nozzle exit velocity and jet diameter (St_D) of 0.51, was chosen for the forced-flow studies. When flow from the REF nozzle was forced at this frequency, coherent vortex ring structures rolled up from the nozzle lip at the forcing frequency. In all "strobed" visualizations of the forced flow, the laser was pulsed at the forcing frequency to "freeze" the flow in space. The flow was filmed on VHS vi-

deotape at 30 frames/s. Therefore, for flow strobed at 364 Hz, each frame of videotape contained approximately 12 superposed images. Time-averaged visualizations were obtained by pulsing the laser at 5600 Hz so that about 187 uncorrelated images were superposed.

The structure of forced, smoke-seeded flow at $Re_D = 19{,}000$ was examined in detail for each of the six nozzle attachments. Both axial and normal slices of the flow are presented where these slices are parallel and perpendicular to the main flow direction, respectively. Four azimuthal orientations and four or more axial positions were examined for each of the nozzles. The results demonstrated that for all of the crown-shaped nozzles, the jet structure differed significantly from that of the axisymmetric reference nozzle. Only a few samples of the visualization results are presented here.

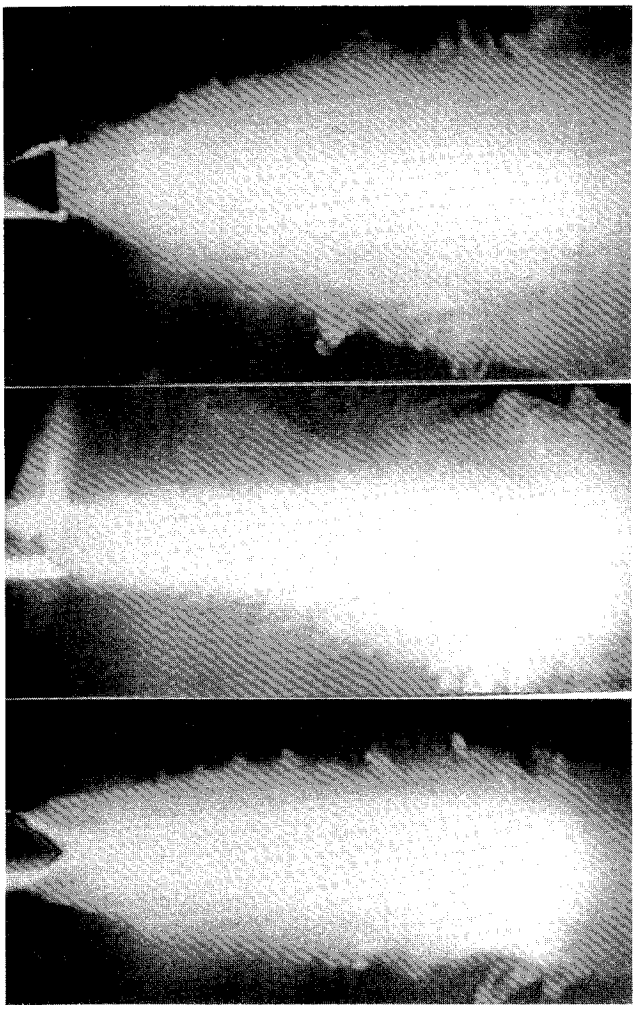

Fig. 10 Time-averaged visualization (2PL nozzle, $St_D = 0.51$, axial cuts, $\beta = 0$, 60, and 90 deg).

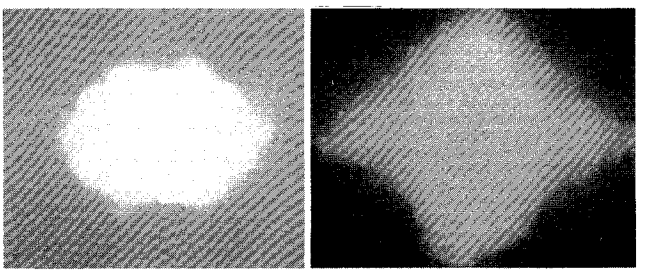

Fig. 11 Time-averaged visualization [2PL nozzle, $St_D = 0.51$, normal cuts, $x/D = 0.82$ (left) and 1.77 (right)].

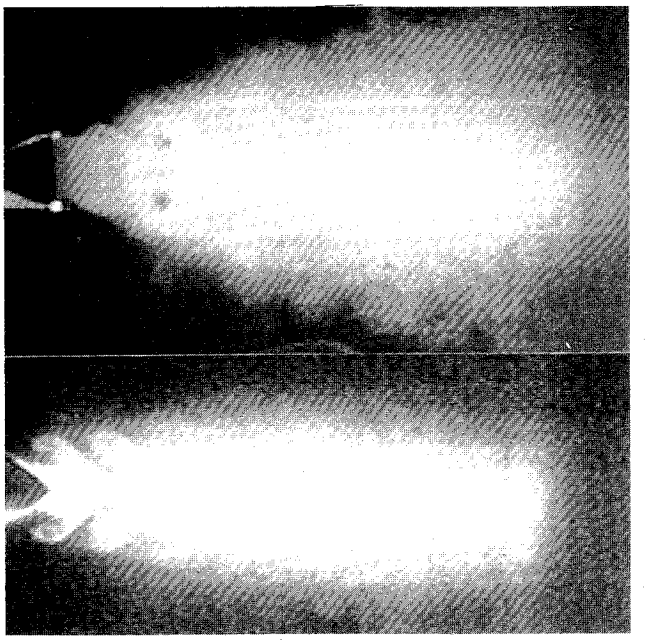

Fig. 12 Strobed visualization (2PL nozzle, $St_D = 0.51$, axial cuts, $\beta = 0$ and 90 deg).

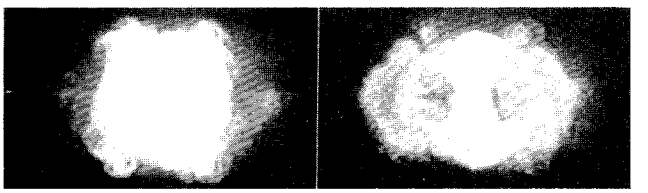

Fig. 13 Strobed visualization (2PL nozzle, $St_D = 0.51$, normal cuts, $x/D = 0.82$).

Figure 10 exhibits time-averaged axial slices of flow from the 2PL nozzle. Three azimuthal orientations are shown. The spreading rate of the smoke-seeded fluid varies markedly with β. The spreading angle measured for $\beta = 0$ deg (the P plane) over the first three diameters is 26 deg, while for $\beta = 90$ deg (the T plane), the spreading angle is 15.5 deg. For $\beta = 60$ deg, the jet spreads hardly at all in the near field. In Fig. 11, time-averaged normal slices of flow from the 2PL nozzle are shown at two axial positions. As in all subsequent figures of normal cuts, the nozzle peaks are aligned vertically with the page. Initially (at $x/D = 0.82$), the greatest spreading of the jet fluid occurs in the T plane. Also at this position, local maxima in the spreading of jet fluid occur on either side of both peaks. Further downstream at $x/D = 1.77$, these maxima have merged in the plane of the peaks. The jet fluid continues to expand sharply in the P plane until at $x/D = 5.88$, the smoke-marked fluid has spread more than twice as far in the P plane as in the I plane, and normal cuts of the flow exhibit a cross-like shape. Beyond this axial location, the jet shape becomes difficult to discern due to the large amount of mixing of smoke-seeded and ambient fluid.

The actual structures present in the flow can be seen in Fig. 12 where two azimuthal orientations of flow at a single forcing phase are shown. The different views depict coherent vortical structures in the flow, but a comparison of the axial positions of the vortex cores shows that the ring structures are *bent* in the shape of the nozzle's downstream edges, i.e., the rings are distorted azimuthally into a zigzag shape. Also, between the vortex rings, the width of the core of unmixed jet fluid is narrower in the T plane than in the REF case indicating a strong entrainment of ambient fluid. In the P plane, on the other hand, the core of unmixed jet fluid appears wider than that in the

REF case, and entrainment between the vortex rings appears reduced.

Figure 13 displays two phase-specific normal cuts of flow from the 2PL nozzle at $x/D = 0.82$. On the left, small, longitudinally oriented secondary structures occur near the plane of the nozzle peaks. These structures are mushroom-shaped indicating that pairs of counter-rotating vortices exist. The videotapes show that the outer vortex of each pair usually dominates and that the fluid between the pair members is directed approximately parallel to the nozzle surface and toward the peaks. In the photograph on the right, ambient fluid is entrained into the jet near the T plane. The smoke-marked fluid present outside of the nozzle perimeter is part of a region possessing azimuthal or primary vorticity. The strongest influx of fluid occurs exactly in the T plane. Outer fluid is directed toward the T plane from both sides so that secondary structures with longitudinal vorticity develop. The direction of longitudinal vorticity in each quadrant matches that of the outer vortices in the previous photograph, and the videotapes show that the inner and outer longitudinal structures are connected. The same types of secondary structures are present up to $x/D = 1.77$, where pairs of the structures appear to merge at the P plane during part of the forcing cycle. Not until this axial location does the inner jet fluid spread significantly beyond the nozzle radius in the P plane. A cartoon illustrating the probable overall jet structure is presented in Fig. 14.

Visualization results from the 4P nozzle are presented in Fig. 15. This nozzle has twice as many peaks as the 2PL nozzle, but half the difference in height between peaks and troughs. Hence, the slopes of the trailing edges of the two nozzles are equivalent. As in the 2PL case, primary vortex ring structures are present. In the 4P case, the rings are not bent but planar. (Note that the ring cores for $\beta = 0$ deg and $\beta = 90$ deg are aligned in x). Time-averaged images show that in this case, smoke-marked fluid spreads even faster in the P plane than in the 2PL case. The mechanism for this spreading is made clear by Fig. 16. At both $x/D = 0.89$ and $x/D = 1.52$, pairs of counter-rotating vortices containing smoke-marked fluid project outward beyond the nozzle peaks. Again in the T planes, ambient fluid is entrained into the jet core. This fluid is also organized into counter-rotating pairs with the inwardly moving fluid rotating away from the T plane. The direction of rotation of this inner fluid in each octant matches that of the fluid in the vortex projecting from the nozzle peak in the same octant. It is again apparent from the videotape that the inner entrained structures are connected to the corresponding outer projecting structures.

Flow from the 2PM nozzle exhibits structures in the P planes similar to those seen in the 4P nozzle (see Fig. 17). Thus, the

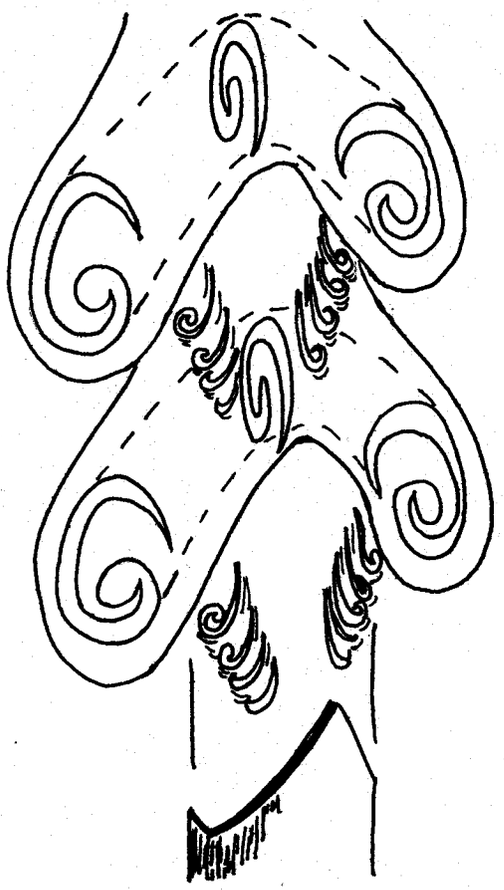

Fig. 14 Cartoon of three-dimensional structure (2PL nozzle).

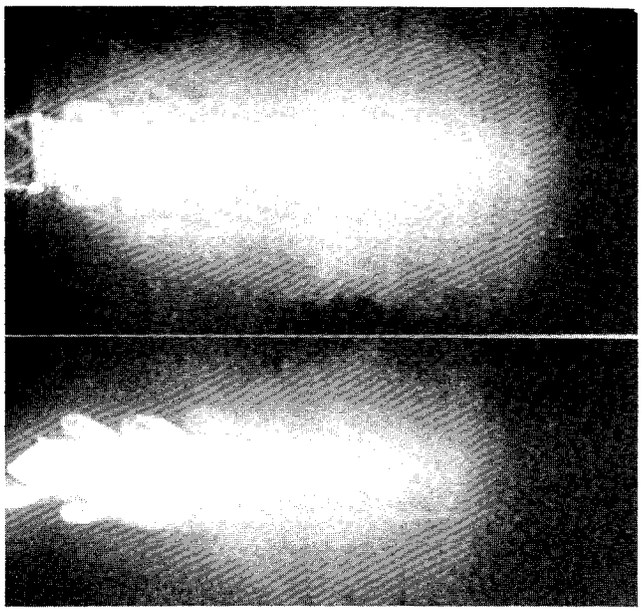

Fig. 15 Strobed visualization (4P nozzle, $St_D = 0.51$, axial cuts, $\beta = 0$ and 45 deg).

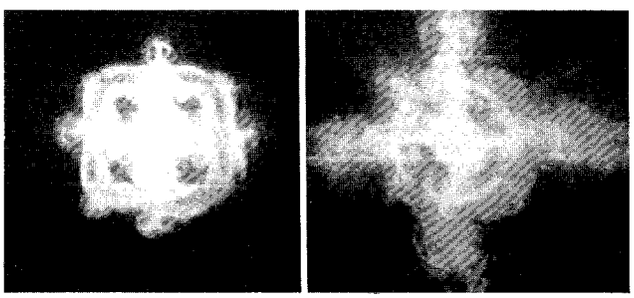

Fig. 16 Strobed visualization [4P nozzle, $St_D = 0.51$, normal cuts, $x/D = 0.89$ (left) and 1.52 (right)].

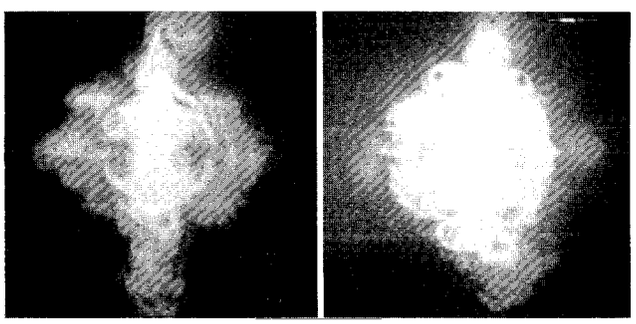

Fig. 17 Strobed visualization (2PM nozzle, $St_D = 0.51$, normal cuts, $x/D = 1.52$).

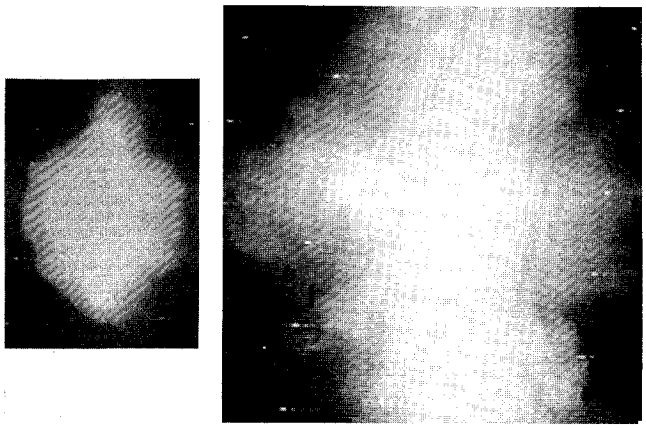

Fig. 18 Time-averaged visualization [2PS nozzle, St_D = 0.51, normal cuts, x/D = 1.40 (left) and 5.20 (right)].

presence of these structures seems dependent on the ratio of tooth length to nozzle diameter rather than on the tooth slope relative to the mean flow direction. It is also interesting to note that longitudinal structures form near the nozzle peaks in addition to the structures centered in the P plane. These structures are very similar to those found in the 2PL case.

Flow from the 2PS nozzle is the final case discussed. Time-averaged normal cuts at two axial positions are shown in Fig. 18. Even though the nozzle deviates only slightly from axisymmetry, the flow is highly asymmetric. At x/D = 5.20, the width of the smoke-marked fluid was measured as 4.8D and 2.4D in the P and T planes, respectively. Thus, asymmetry persists through the jet near field. The longitudinal structures in this case form at more random azimuthal locations compared with the 2PL or 2PM cases, although preferred locations are observed.

Before concluding this section, we note that the measured spreading angles in the time-averaged forced flow were larger than those in the unforced flow. These results suggest that the types of structures that enhance jet spreading in the forced flow are present at most intermittently in the unforced flow. When the jet is forced at a higher frequency (St_D = 0.78), flow from the 2PL nozzle appears more axisymmetric than for St_D = 0.51, e.g., enhanced spreading in the P and T planes is less pronounced. Although coherent longitudinal structures form around the nozzle perimeter, they do not lock on to a specific azimuthal position as strongly as for St_D = 0.51. Also, the regions of entrained ambient fluid near the nozzle's T planes are smaller for St_D = 0.78. Thus, the smaller, more tightly spaced primary structures forming in the higher frequency forced jet seem to inhibit the formation of the repeatable organized longitudinal structures seen in the lower frequency case.

Discussion

It is apparent from the flow-visualization studies and hot-wire measurements that the crown-shaped nozzles have a strong effect on near-field jet structure in both forced and unforced flow. The studies on forced flow indicate that the crown-shaped nozzles tend to both increase and organize the mixing of inner jet fluid and outer ambient fluid. In round jets, it has been shown (see Monkewitz et al.,[9] for example) that smaller scale mixing between jet and ambient fluid occurs due to azimuthal irregularities in the jet's primary vortex ring structures. Widnall instabilities (see Widnall et al.[10]) cause waviness in the rings. The waves become amplified with increasing downstream distance so that secondary longitudinally oriented structures form. Mixing caused by the formation and development of these structures occurs at random locations around the jet circumference.

Since the crown-shaped nozzles are not axisymmetric, azimuthal instabilities and hence secondary structures occur at specific nonrandom locations. The most striking flow feature caused by the crown-shaped nozzles is an increased level of entrainment in the regions near the nozzles' trough planes. In all cases, unmarked ambient fluid penetrates into the jet core in these planes and forms pairs of counter-rotating longitudinal structures. This fluid penetrates significantly deeper into the jet core than ambient fluid rolling up in the primary vortex rings. The ambient fluid entrained into the jet core near the trough planes is also present over a greater portion of the forcing cycle than the ambient fluid in the primary ring cores implying that the volume of fluid entrained is substantial. The preferential induction of fluid in the trough planes could possibly be explained by local pressure minima occurring once per forcing cycle at the trough locations. Where a pressure minimum would normally be spread around the entire circumference of a round nozzle exit, it is concentrated within a small region for a crown-shaped nozzle and hence is likely to cause a stronger local perturbation. This idea is illustrated in Fig. 19. Outer fluid, which would normally be entrained parallel to the mean flow, tends to be pulled in toward the troughs from both sides inducing rotation away from the troughs once the fluid reaches the jet interior. Detailed velocity measurements in the normal plane would be required to confirm this hypothesis.

Since ambient fluid close to the nozzle exit is induced to move toward the trough planes, it is also induced to move away from the peak planes. Thus, the inner jet fluid at the peak plane tends to move radially outward. The outflow at these points helps induce longitudinal structures near the peak planes with the same direction of rotation as those forming inside the jet near the trough planes. In all cases, the inner and outer structures appear to connect to one another. For all four crown-shaped nozzles described earlier in the Forced Flow section, strong ejection of inner (smoke-marked) fluid was observed in the peak planes due to structures with longitudinal vorticity. Therefore, in the P plane, mixing of inner and ambient fluid took place over a wider radial range than in the round jet. We can also say that the inner fluid was dispersed farther in this plane in the crown-shaped jets than it was in a round jet. Thus, it seems that the jagged nozzles can be effective not only to increase entrainment and mixing near the jet axis, but also to increase or to distort the overall distribution area of the original jet fluid. Also, the nozzle geometries allow the azimuthal positions of increased spreading and increased entrainment to be chosen arbitrarily.

Of the crown-shaped cases discussed in the previous section, the two most similar are the 4P and 2PM. Both of these cases exhibit very strong spreading in the P planes due to ejection of jet core fluid by longitudinal structures. The sizes and shapes of the structures are similar in both cases. This similarity suggests that the tooth length must be critical to the formation of these structures downstream of the nozzle peaks.

When the 2PL and 4P cases are compared, an apparent contradiction arises. The slopes of the trailing edges of these two nozzles are equivalent, but the shapes of the primary vortex rings are different. In the 2PL case, the primary vortex rings

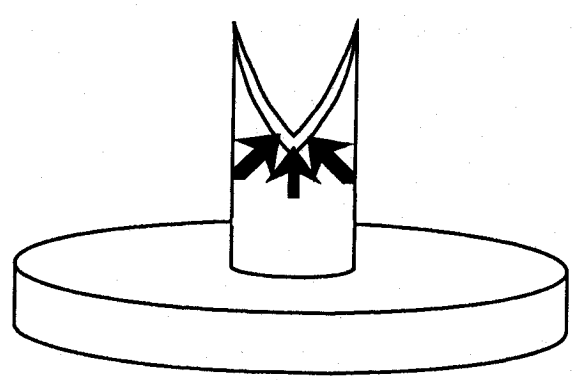

Fig. 19 Paths of entrainment flow into jet core.

are distorted such that the cores in the P plane are centered about $0.9D$ downstream of the cores in the T plane. It appears that the rings are bent into the shape of the nozzle's trailing edges. In the 4P case, however, the primary rings are planar. Thus, it seems that competing mechanisms are present that encourage alignment of the primary vortex rings either parallel to the nozzle exit or perpendicular to the mean flow direction and that the tooth slope and initial shear-layer thickness (assumed as approximately the same for both cases) are not the only parameters important in determining the primary vortex shape. Other important parameters are probably the normalized tooth length and the Strouhal number (which determines the vortex ring spacing). The conditions $Re_D = 19{,}000$ and $St_D = 0.51$ yielded an axial ring spacing of about $1D$. Therefore, the ring spacing is about equal to the tooth length for the 2PL nozzle and about twice the tooth length for the 4P nozzle. In the 4P case, the axial positions of the nozzle's trailing edges in the T and P planes are separated by about one-half of a forcing cycle. Therefore, the flow downstream of the troughs is 180 deg out of phase with the flow downstream of the peaks. Rings bent into the shape of the nozzle exit are discouraged from forming, and planar rings form perpendicular to the jet axis instead. In the 2PL case, the waves rolling up off the nozzle lip in the T and P planes, respectively, are in phase. Although it would seem that planar rings are possible, the mechanism encouraging the primary vorticity to develop parallel to the nozzle's trailing edges dominates so that bent structures form.

The comparisons made above are based on flow forced at $St_D = 0.51$, where primary rings of a specific size are generated. When the flow is forced at a higher frequency ($St_D = 0.78$), smaller rings form, and differences in the flow structures are observed. In the higher-frequency case, the spacing between the primary vortex rings is about $0.6D$. Hence, the flow immediately downstream of the peaks and troughs is almost 180 deg out of phase. Therefore, the differences in flow structure observed in this case cannot be attributed only to the smaller primary vortex rings that form but also to the relationship between the size of the primary vortex rings and the nozzle tooth length.

Conclusions

Hot-wire and flow-visualization studies on unforced flow from crown-shaped nozzles show that the nozzles can cause significant deviations from axisymmetry. Studies of the repeatable structures generated under forced-flow conditions reveal some probable mechanisms for these deviations. The nozzles tend to inject longitudinal vorticity into the flow. In the trough planes, this vorticity causes increased entrainment of ambient fluid into the jet core. In the peak planes, some nozzles eject inner jet fluid through longitudinal structures.

Although it was originally hypothesized that nozzles with longer tooth lengths would cause greater deviations from axisymmetry in the flow than nozzles with shorter tooth lengths, this was not necessarily the result. In the forced-flow studies, the 2PM and 4P nozzles exhibited faster spreading in the P plane than the 2PL nozzle, and the 2PS nozzle spread at about the same angle in the P plane as the 2PL. Thus, for a control objective of dispersing jet fluid over an increased radial distance, only a small tooth length is necessary. However, if strong entrainment into the jet core in the jet near field is desired, a large tooth length is appropriate.

Acknowledgments

This work was funded by the Electric Power Research Institute under Contract RP 8005-2 monitored by George Offen. The first author was supported by fellowships from the Link Foundation and the American Association of University Women.

References

[1]Ho, C. M., and Gutmark, E., "Vortex Induction and Mass Entrainment in a Small-Aspect-Ratio Elliptic Jet," *Journal of Fluid Mechanics*, Vol. 179, No. 2, June 1987, pp. 383–405.

[2]Schadow, K. C., Gutmark, E., Parr, D. M., and Wilson, K. J., "Selective Control of Flow Coherence in Triangular Jets," *Experiments in Fluids*, Vol. 6, 1988, pp. 129–135.

[3]Bradbury, L. J. S., and Khadem, A. H., "The Distortion of a Jet by Tabs," *Journal of Fluid Mechanics*, Vol. 70, Aug. 1975, pp. 801–813.

[4]Kibens, V., and Wlezien, R. W., "Active Control of Jets from Indeterminate-Origin Nozzles," AIAA Paper 85-0542, Boulder, CO, March 1985.

[5]Wlezien, R. W., and Kibens, V., "Passive Control of Jets with Indeterminate Origins," *AIAA Journal*, Vol. 24, No. 8, 1986, pp. 1263–1270.

[6]Krishnappa, G., and Csanady, G. T., "An Experimental Investigation of the Composition of Jet Noise," *Journal of Fluid Mechanics*, Vol. 37, June 1969, pp. 149–159.

[7]Longmire, E. K., and Eaton, J. K., "Structure and Control of a Particle-Laden Jet," Thermosciences Div., Dept. of Mechanical Engineering, Stanford Univ., MD-58, Stanford, CA, Sept. 1990.

[8]Tutu, N. K., and Chevray, R., "Cross-Wire Anemometry in High Intensity Turbulence," *Journal of Fluid Mechanics*, Vol. 71, Oct. 1975, pp. 785–800.

[9]Monkewitz, P. A., Lehmann, B., Barsikow, B., and Bechert, D. W., "The Spreading of Self-Excited Hot Jets by Side Jets," *Physics of Fluids A*, Vol. 1, No. 3, 1989, pp. 446–448.

[10]Widnall, S. E., Bliss, D. B., and Tsai, C.-Y., "The Instability of Short Waves on a Vortex Ring," *Journal of Fluid Mechanics*, Vol. 66, Oct. 1974, pp. 35–47.